THE ASTROPHYSICAL JOURNAL, 225:843–856, 1978 November 1

RADIO OBSERVATIONS OF INTERSTELLAR CN TOWARD DIFFUSE CLOUDS, DARK CLOUDS, BLACK CLOUDS, AND CIRCUMSTELLAR CLOUDS

MARK ALLEN
NASA Goddard Institute for Space Studies
AND
G. R. KNAPP
Owens Valley Radio Observatory, California Institute of Technology
Received 1977 November 28; accepted 1978 May 8

ABSTRACT

Emission at 113 GHz from the CN molecule has been searched for in a large number of interstellar regions, primarily dark dust clouds. Lines have been detected in four dark clouds, the first time CN has been observed in this type of object. Comparative CO observations were also performed. The CN/CO abundance ratio varies from cloud to cloud, even among objects which are apparently otherwise similar. This variation suggests that the chemistry of dark clouds may be time-dependent. A previously reported detection of CN emission from a diffuse cloud was not confirmed. Several black clouds and circumstellar clouds were reobserved to obtain better line parameters and to serve as comparative interstellar chemical systems.

Subject headings: interstellar: molecules — interstellar: abundances — stars: circumstellar shells

I. INTRODUCTION

Radio-wavelength emission from many species of molecules has been detected in a variety of interstellar environments (Zuckerman and Palmer 1974): diffuse clouds, in which dissociation and ionization by photons with energies less than 13.6 eV strongly influence the chemistry; cold dark clouds, whose cores may be isolated from intense localized sources of radiation; larger warmer black clouds (this notation was suggested by Scoville 1972), whose molecular regions are spatially associated with strong infrared and/or H II regions; and circumstellar clouds, probably the results of outflow from the atmospheres of evolved stars. Because the physical conditions vary so widely among these different cloud types, Turner (1974) has suggested that the chemical processes producing the observed molecules may likewise vary. Observations of chemical abundances in these different cloud types may then lead to an elucidation of the physical and chemical processes involved.

Allen and Robinson (1977, hereafter AR77) suggest that it might be easiest to understand the chemistry of dark clouds. The low kinetic temperatures (typically, kinetic temperature $T_k \sim 10$ K) and weak radiation fields in these objects severely restrict the range and type of physical and chemical processes which might be important. Interestingly, the various models of dark cloud chemistry that have been developed differ in the type of reactions employed and/or the approach adopted in analyzing the rate equations. Herbst and Klemperer (1973, hereafter HK) present a gas-phase model, utilizing mainly ion-molecule reactions and including a large number of chemical species. They propose that the interstellar clouds have reached chemical steady state, though not thermodynamic equilibrium, so that the observed abundances are simply a function of cloud density. Several recent gas-phase models incorporating a more limited number of species (Oppenheimer and Dalgarno 1975; Langer and Glassgold 1976; Gerola and Glassgold 1978) and two on the scale of HK (Prasad and Huntress 1978, hereafter PH; Iglesias 1977, hereafter IG) suggest that the abundances of many interstellar molecules vary significantly on astrophysically relevant time scales. Employing a radically different kind of chemistry—reactions on grain surfaces—the model of AR77 also suggests that the observed molecular abundances reflect both the cloud density and the cloud age. In an earlier paper (Allen and Robinson 1976, hereafter AR76), such an analysis is applied to the abundance of H I in dark clouds to explain the variation in the atomic hydrogen content of clouds with similar total extinctions. Most recently, Pickles and Williams (1977) present the results of steady-state calculations involving both gas-phase and surface reactions.

This paper reports observations of the free radical CN in a variety of types of interstellar clouds, mostly dark clouds, in an attempt to examine and compare the predictions of models which include CN chemistry. The CN radical is one of the more abundant heavy molecules in these models and is a highly reactive species, so that its abundance may vary significantly from cloud to cloud if interstellar clouds are chemically dynamic on relevant time scales.

Turner and Gammon (1975, hereafter TG) observe CN in a large number of interstellar clouds, but not in dark clouds, although several were searched. In the present work, we report the detection of CN in four dark clouds, adding this molecule to the ever-growing list of molecules observed in dark clouds, once thought to be relatively uninteresting from a chemical standpoint.

Since radio spectral line observations lead directly to measurements of column density, it is easier to measure the relative concentrations of two observable molecules. We therefore used carbon monoxide as a comparison molecule, since it is easy to detect and provides a relatively good measure of the total gas content of a cloud. Various theories suggest, and observations (e.g., Dickman 1977) confirm, that a fairly constant fraction of the carbon content of dark clouds is in the form of carbon monoxide (assuming that the $^{13}CO/^{12}CO$ abundance ratio is invariant). Carbon monoxide is also especially good as the comparison molecule because its concentration is relatively independent of cloud age in all the time-dependent models.

In addition to our observations of dark clouds, we searched for, and in some cases detected, CN in the other types of interstellar clouds previously mentioned. This was done both to clarify some of the observations of TG and to attempt to detect variations in the CN/CO relative abundances which might reflect differences in cloud chemistry in different environments.

II. OBSERVATIONS AND DATA REDUCTION

a) *Observations and Calculation of Line Parameters*

The molecules in our program were $^{12}C^{16}O$ (115 GHz, hereafter CO), $^{13}C^{16}O$ (110 GHz), and $^{12}C^{14}N$ (113 GHz, hereafter CN). The specific transitions observed are listed in Table 1. For CN, the relative intensities of the hyperfine components which fell within our bandpass are listed. The CN frequencies are derived from two different sources, as given in the notes to Table 1.

The observations were made in 1976 October with the National Radio Astronomy Observatory's[1] 11 meter (36 foot) telescope at Kitt Peak, Arizona. The telescope half-power beamwidth is ~65″, the aperture efficiency ~34%, and the beam efficiency ~65%. The NRAO cooled-mixer Cassegrain receiver was used, and its effective single-sideband system temperature was ~1200 K. (This contains contributions from the atmosphere, etc.) The back-end consisted of two 256-channel filter banks, centered at the same frequency, but with different resolutions. Depending on the expected line width of the source, filter banks with resolutions of 500 kHz per channel (≡1.32 km s^{-1} at 113.5 GHz), 250 kHz (0.66 km s^{-1}), and 100 kHz (0.26 km s^{-1}) were used.

To ensure the best baselines possible, the observations were carried out in a position-switching mode. For small sources, the reference position was 30′ from the source in azimuth or right ascension. For the more extended clouds, a reference position near each source was chosen to be relatively free of dust (and by assumption molecules) by examination of the Palomar Observatory Sky Survey prints. Total integration times of up to several hours per point were accumulated for the CN observations; for the CO observations, total times of 5 minutes per point were used. Removal of linear baselines from the data was usually sufficient. However, for a few observations, removal of higher-order baselines was sometimes necessary; the poorer baselines were due to variable weather conditions or to the large angular distance between the source and reference positions in some cases. The presence of nonlinear baselines does not affect our data in any serious way, however, since most of the observed lines were very narrow, occupying only a few channels. Except where noted, the spectral line parameters were calculated from least-squares fitting of Gaussian functions to the data after baseline removal. The values for the peak temperature, T_A^*, and for ΔV, the velocity full width at half-power, were corrected for channel dilution. The temperatures T_A^* are in terms of the Rayleigh-Jeans equivalent brightness temperature measured by a lossless antenna above the atmosphere. The temperature scales were calibrated using an oscillating vane (see Ulich and Hass 1976), and, to improve the reliability of the

[1] The National Radio Astronomy Observatory is operated by Associated Universities, Inc., under contract with the National Science Foundation.

TABLE 1

MOLECULAR TRANSITIONS OBSERVED

Molecule	Transition	Frequency (MHz)	Relative Intensity*
$^{12}C^{16}O$.......	$J = 0\text{–}1$	115,271.20	...
$^{13}C^{16}O$.......	$J = 0\text{–}1$	110,201.37	...
$^{12}C^{14}N$.......	$NJF = 0, \frac{1}{2}, \frac{1}{2}\text{–}1, 3/2, 3/2$	113,488.14†	10
	$NJF = 0, \frac{1}{2}, 3/2\text{–}1, 3/2, 5/2$	113,490.99†	27
	$NJF = 0, \frac{1}{2}, \frac{1}{2}\text{–}1, 3/2, \frac{1}{2}$	113,499.64†	8
	$NJF = 0, \frac{1}{2}, 3/2\text{–}1, 3/2, 3/2$	113,508.93†	8
	$NJF = 0, \frac{1}{2}, 3/2\text{–}1, 3/2, \frac{1}{2}$	113,520.24‡	1

* TG.

† Average of frequencies determined via methods A and B (Dixon and Woods 1977).

‡ Downward correction of frequency determined by TG, approximately in line with other corrections determined by Dixon and Woods 1977.

1978ApJ...225..843A

TABLE 2

DARK CLOUD AND DIFFUSE CLOUD CO AND CN OBSERVATIONAL RESULTS

Source	α_{1950}	δ_{1950}	l^{II}	b^{II}	^{12}CO (J = 1–0) T_A^* (K)	V_{LSR} (km s^{-1})	ΔV (km s^{-1})	^{13}CO (J = 1–0) T_A^* (K)	V_{LSR} (km s^{-1})	ΔV (km s^{-1})	CN (NJF = 1, 3/2, 5/2–0, ½, 3/2) T_A^* (K)	V_{LSR} (km s^{-1})	ΔV (km s^{-1})	CN (NJF = 1, 3/2, 3/2–0, ½, ½) T_A^* (K)	V_{LSR} (km s^{-1})	ΔV (km s^{-1})
a) Dark Clouds																
L1333	02h21m00s0	75°15′00″	128°88	13.71	4.46*	3.2*	2.0*	3.44*	3.6*	0.8*	< 0.35	...	...	...	...	...
IC 1848-1	02 59 22.2	60 16 00	138.50	1.64	11.24	−38.8	3.3	2.22	−38.0	2.7	0.37	−38.3	3.2	< 0.33	...	...
					(0.37)	(0.1)	(0.1)	(0.12)	(0.1)	(0.2)	(0.05)	(0.2)	(0.5)	...	...	...
L1551	04 28 30.0	18 00 18	178.92	−20.09	8.61	6.4	1.8	4.87	6.8	1.0	< 0.52	...	...	...	...	...
					(0.53)	(0.1)	(0.1)	(0.21)	(< 0.1)	(0.1)	...	...	...	...	...	...
					3.79	−1.1	3.3	< 0.76	...	...	...	...	...	...	...	...
					(0.39)	(0.2)	(0.4)	...	...	...	...	...	...	...	...	...
L1529 (Taurus dark	04 29 42.9	24 16 54	174.06	−15.85	7.58	5.9	2.8	4.80	6.6	1.5	0.47‡	6.3	0.7	0.39‡	6.3	0.7
cloud)					(0.45)	(0.1)	(0.2)	(0.16)	(< 0.1)	(0.1)	(0.07)	(0.1)	(0.1)	(0.07)	(0.1)	(0.2)
L1534 (Heiles Cloud 2,	04 38 38.9	25 34 59	174.39	−13.45	7.06	5.8	2.6	2.82	6.1	1.9	< 0.45	...	...	...	...	...
Taurus dark cloud)					(0.50)	(0.1)	(0.2)	(0.13)	(0.1)	(0.1)	...	...	...	...	...	...
L1552	05 14 35.9	25 59 59	179.04	−6.76	7.21	7.5	0.9	3.21	7.9	1.0	< 0.41	...	...	...	...	...
					(0.71)	(0.1)	(0.1)	(0.21)	(< 0.1)	(0.1)	...	...	...	...	...	...
Ori-I-2	05 35 33.0	−01 46 40	205.95	−17.09	9.57	12.7	1.5	3.69	13.2	1.1	0.45§	13.0	1.2	0.38§	13.1	0.9
					(0.60)	(0.1)	(0.1)	(0.20)	(< 0.1)	(0.1)	(0.08)	(0.1)	(0.3)	(0.10)	(0.1)	(0.3)
L1622	05 51 51.6	01 47 42	204.70	−11.80	13.75	1.0	1.6	6.67	1.4	1.1	< 0.45	...	...	...	...	...
					(0.55)	(< 0.1)	(0.1)	(0.22)	(< 0.1)	(< 0.1)	...	...	...	...	...	...
					3.46	10.5	1.2	< 0.94	...	...	...	...	...	...	...	...
					(0.66)	(0.1)	(0.3)	...	...	...	...	...	...	...	...	...
B227	06 04 31.0	19 28 30	190.69	−0.46	6.06	−0.5	1.6	2.57	0.0	1.2	< 0.33	...	...	...	...	...
					(0.43)	(0.1)	(0.2)	(0.21)	(0.1)	(0.1)	...	...	...	...	...	...
					4.03	8.2	1.7	< 0.90	...	..	...	...	...	...	...	...
					(0.42)	(0.1)	(0.2)	...	...	...	...	...	...	...	...	...
Monoceros (Bok globule	06 38 44.0	09 24 12	203.47	2.06	10.62	8.2	2.2	4.63	8.4	1.9	< 0.26	...	...	...	...	...
near NGC 2264)					(1.70)	(0.1)	(0.2)	(0.15)	(< 0.1)	(0.1)	...	...	...	...	...	...
					7.95	5.8	3.2	2.29	5.4	1.5	...	...	...	...	...	...
					(0.68)	(0.3)	(0.5)	(0.17)	(0.1)	(0.1)	...	...	...	...	...	...
L134	15 51 00.0	−04 26 57	4.23	35.78	4.69	2.4	0.6	3.70	3.1	1.0	< 0.50	...	...	...	...	...
					(1.09)	(0.1)	(0.2)	(0.32)	(0.1)	(0.1)	...	...	...	...	...	...
L134N (L183)	15 51 30.0	−02 43 31	6.01	36.75	4.33	2.2	1.3	2.56	3.0	1.2	< 0.73	...	...	...	...	...
					(0.76)	(0.1)	(0.3)	(0.25)	(0.1)	(0.1)	...	...	...	...	...	...
ρ Oph (Heiles Cloud 4,	16 24 07.9	−24 28 01	353.05	16.67	9.1*	3.5*	4.1*	1.92	3.8	3.6	< 0.38	...	...	...	...	...
L1681)								(0.27)	(0.2)	(0.6)	...	...	...	...	...	...
Kh 3	18 52 38.9	02 21 35	35.51	0.28	3.18†	12.6†	5.0†	0.48†	12.7†	5.3†	< 0.45	...	...	...	...	...
					(0.47)	(0.4)	(0.9)	(0.08)	(0.4)	(0.9)	...	...	...	...	...	...
B335 (L663)	19 34 34.0	07 27 00	44.92	−6.56	4.61	8.0	1.3	3.12	8.5	0.6	0.31	8.4	0.9	< 0.20	...	...
					(0.46)	(0.1)	(0.2)	(0.29)	(< 0.1)	(0.1)	(0.06)	(0.1)	(0.2)	...	...	...
Cep C	23 03 21.0	62 12 22	111.02	2.08	11.27	−10.5	3.4	5.23	−10.0	2.0	< 0.43	...	...	...	...	...
					(0.35)	(0.1)	(0.1)	(0.14)	(< 0.1)	(0.1)	...	...	...	...	...	...
b) Diffuse Cloud																
HD 21483	03 25 41.9	30 12 11	158.87	−21.30	6.93	5.7	2.1	1.57	5.8	1.5	< 0.35	...	...	...	...	...
					(0.35)	(0.1)	(0.1)	(0.16)	(0.1)	(0.2)	...	...	...	...	...	...

* Determined without using Gaussian least-squares fits.
† Data from 250 kHz filters.
‡ Baseline rms = 0.08 K.
§ Baseline rms = 0.13 K.

TABLE 3

DARK CLOUD AND DIFFUSE CLOUD CO AND CN NEGATIVE RESULTS

SOURCE	α_{1950}	δ_{1950}	l^{II}	b^{II}	^{12}CO (J = 1–0) T_A^* (K)	^{12}CO (J = 1–0) V_{LSR} Range Searched (km s^{-1})	CN (NJF = 1, 3/2, 5/2–0, ½, 3/2) T_A^* (K)	CN (NJF = 1, 3/2, 5/2–0, ½, 3/2) V_{LSR} Range Searched (km s^{-1})
HD 154368 (diffuse cloud)........	$17^h03^m08^s.0$	−35°23′05″	349°.97	3°.22	< 6.56	−24.2 → 42.2	< 1.04	−42.3 → 23.9
L915 (dark cloud)...............	20 43 35.9	42 54 59	83.01	0.09	< 2.31	−33.2 → 33.2	< 0.44	−19.9 → 40.9
55 Cyg (diffuse cloud)............	20 47 14.0	45 55 11	85.75	1.49	...	...	< 0.42	−45.2 → 15.9

calibration, an image sideband rejection filter was used (Wannier *et al.* 1976*a*). The temperature calibration was checked by observations of Orion A, whose brightness temperatures in the CO and ^{13}CO lines are 60 K and 9.3 K (Ulich and Haas 1976).

We were mostly interested in dark cloud chemistry, and the selection criteria for the clouds to be observed were various. Because the model of AR77 predicts a possible correlation between the CN and H I abundances, a number of dark clouds were chosen from the H I survey of Knapp (1974). Other dark clouds were selected because "high excitation" molecules, such as CS (Martin and Barrett 1975), were detected in them, showing that the densities may be sufficient to excite CN to an observable degree if the column density is sufficiently large. Several diffuse clouds were observed, since the detection of CN in two such clouds by TG suggested the presence of interesting chemical phenomena. Accordingly, we reobserved the two positions of TG and several other diffuse clouds in which there might be a sufficient amount of gas for CN to be detected (see Knapp and Jura 1976). And to round out our observations, we observed the two most popular black clouds (Orion A and Sgr B2) and the two most popular circumstellar clouds (IRC +10216 and CIT 6).

The results of our CO and CN observations of dark and diffuse clouds are given in Tables 2 and 3, and in Figure 1. The peak temperature T_A*, the velocity[2] $V_{\rm LSR}$ and the velocity width ΔV are given for the CO, the ^{13}CO, and the strongest CN lines; the errors quoted are the formal 1 σ errors resulting from the least-squares fitting of Gaussian profiles to the data. The CN negative results are listed as 3 σ upper limits to T_A*. Except where noted, the data from the 100 kHz filter banks were used. In some CO spectra, several Gaussian functions (corresponding to different velocity components) were required to fit an asymmetric line profile; no *a priori* constraints were placed on the possible values for the line parameters. The CN negative results for clouds in which CO was not detected or CO observations were unavailable are listed in Table 3. Finally, we present in Figure 1 the observed CN line profiles for the four dark clouds in which emission was detected.

[2] Throughout this paper the velocity is expressed relative to the local standard of rest (LSR).

The widths of lines emitted in black clouds and circumstellar clouds are generally much larger than those in dark clouds, resulting in a blending of the different hyperfine components of the N = 1–0 CN transition. The CN profiles for these clouds were therefore synthesized with multiple Gaussian components. The Gaussian function for each hyperfine component was constrained such that the spacings between the Gaussians and their relative intensities were as given in Table 1 and the half-widths of all the components were equal. The observed profiles, and the Gaussian fits, are shown in Figure 2 for the observations toward Orion A, Sgr B2 (OH), IRC +10216, and CIT 6. It can be seen that, given the low signal-to-noise ratio in some spectra, satisfactory fits resulted in all cases. The calculated line parameters are presented in Table 4; except where noted, the data from the 250 kHz filters were used.

b) Calculation of CO *and* CN *Column Densities*

When both the CO and ^{13}CO molecules are detected in a dark or diffuse cloud, the total column density $N(^{13}\mathrm{CO})$ can be simply calculated assuming local thermodynamic equilibrium (LTE); such a procedure will result in an underestimate of the true value of $N(^{13}\mathrm{CO})$ by less than a factor of 2 (Dickman 1975). The LTE approximation assumes that (1) the CO line is optically thick, (2) the excitation temperatures T_{01} of the CO and ^{13}CO transitions are equal, and (3) the source fills the telescope beam. Then the peak ^{13}CO optical depth, $\tau(^{13}\mathrm{CO})$, can be determined from the relation

$$T_A^*(^{13}\mathrm{CO}) = \{J(T_{01}) - J(T_{\rm bg})\}\{1 - \exp[-\tau(^{13}\mathrm{CO})]\} \quad (1)$$

and

$$T_A^*(^{12}\mathrm{CO}) = J(T_{01}) - J(T_{\rm bg}) , \quad (2)$$

TABLE 4

BLACK CLOUD AND CIRCUMSTELLAR CLOUD CN OBSERVATIONAL RESULTS

Source	α_{1950}	δ_{1950}	$l^{\rm II}$	$b^{\rm II}$	CN (NJF = 1, 3/2, 5/2–0, ½, 3/2) T_A* (K)	$V_{\rm LSR}$ (km s^{-1})	ΔV (km s^{-1})
a) Black clouds:							
Ori A	5h32m47s.0	−05°24′21″	208°.99	−19°.38	4.25* (0.27)	9.3* (0.1)	3.5* (0.1)
Sgr B2 (OH)	17 44 11.0	−28 22 30	0.66	−0.04	0.45 (0.09)	89.6 (0.9)	18.4 (1.9)
b) Circumstellar clouds:							
IRC +10216	09 45 15.0	13 30 39	221.45	45.06	0.89 (0.01)	−23.1 (0.7)	27.7 (1.7)
CIT 6 (IRC +30219)	10 13 12.0	30 49 24	197.71	55.97	0.11 (0.03)	1.9 (1.5)	23.4 (3.5)

* Data from 100 kHz filters.

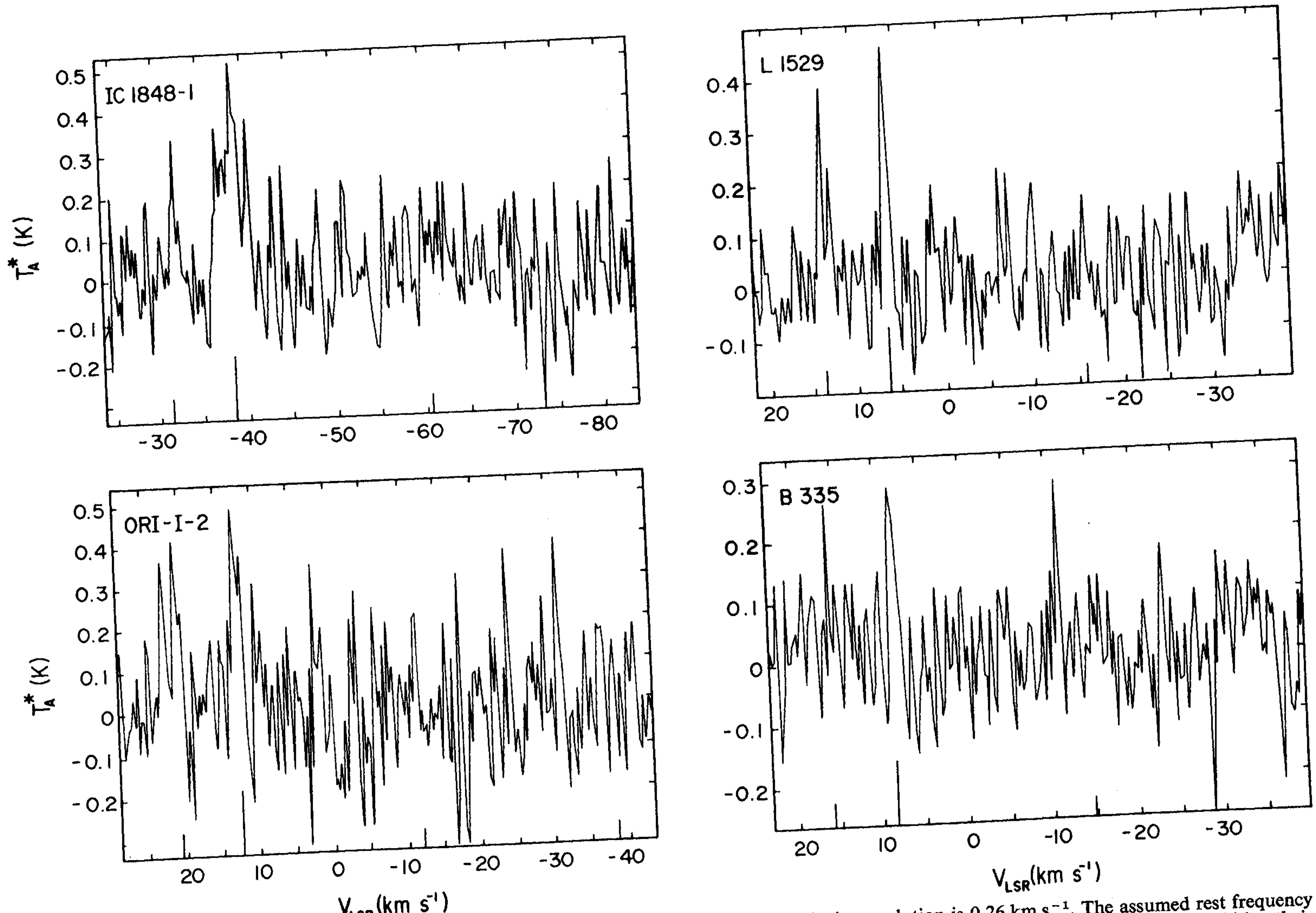

FIG. 1.—CN spectra for the four dark clouds in which the molecule was detected. The velocity resolution is 0.26 km s^{-1}. The assumed rest frequency is that of the strongest hyperfine component, 113,490.99 MHz. The vertical lines indicate the positions where the hyperfine components should be, their LTE relative intensities being reflected by the heights of the lines.

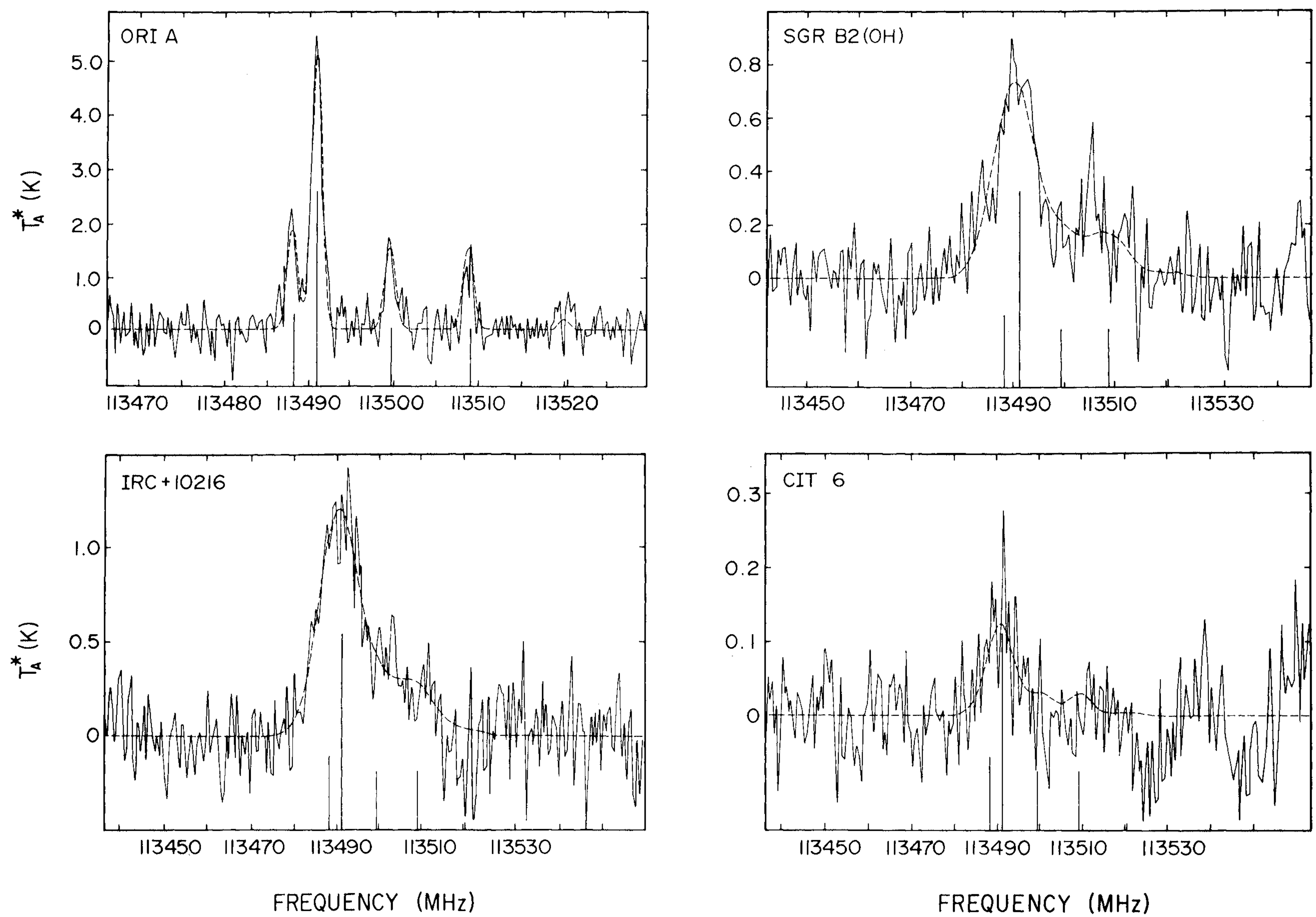

FIG. 2.—CN profiles for the black clouds and circumstellar clouds. Also shown are the synthetic spectra (*dashed lines*) calculated as described in the text and the center position and adopted relative intensity of the Gaussian function for each of the hyperfine components. The velocity resolution is 1.32 km s^{-1}, except in the case of Ori A, in which it is 0.66 km s^{-1}. The abscissae show the rest frequencies calculated assuming the source radial velocity to be as given in Table 4.

where

$$J(T) = \frac{h\nu}{k}\left[\exp\left(\frac{h\nu}{kT}\right) - 1\right]^{-1}, \quad (3)$$

ν is the frequency of the relevant rotational transition, and T_{bg} the background radiation temperature, which at these frequencies is the 2.7 K cosmic blackbody microwave radiation field. The total column density $N(^{13}CO)$ is then derived from $\tau(^{13}CO)$ as follows:

$$N(^{13}CO) = \frac{6.39 \times 10^{14} Q(T_{01}) \Delta V(^{13}CO) \tau(^{13}CO)}{1 - \exp(-h\nu/kT_{01})}, \quad (4)$$

where $Q(T_{01})$ is the partition function and $\Delta V(^{13}CO)$ is in units of km s^{-1}. Finally, we assume that $N(^{12}CO)/N(^{13}CO) = 89$ (the solar system ratio of $^{12}C/^{13}C$), which may be a factor of 2 too large for the general interstellar medium (Wannier *et al.* 1976*b*).

In the cases of dark clouds in which CO, but not ^{13}CO, was detected, we assumed that the CO lines are optically thin, and obtained N(CO) directly from the line formation models of Lucas (1974) for $n(H_2) = 10^3$ cm^{-3} and $T_k = 10$ K. However, the results of Scoville and Solomon (1974) suggest that CO can be optically thick even when ^{13}CO is undetectable; the column densities derived under this assumption using the same cloud parameters as before can be about an order of magnitude larger than the corresponding Lucas values.

For the black and circumstellar clouds, the CO column densities were obtained from equations (1)–(4) using published CO and ^{13}CO observations (by Ulich and Haas 1976 for Orion A; by Scoville, Solomon, and Penzias 1975 for Sgr B2; by Kuiper *et al.* 1976 for IRC +10216; and by Mufson and Liszt 1975 for CIT 6). In the case of CIT 6, the source is known to be smaller than the telescope beam (Mufson and Liszt 1975); however, the value of N(CO) was not corrected for beam size to remain consistent with our calculation of N(CN).

A simple procedure was employed in calculating N(CN). In the case where the CN lines are optically thin, the column density is given by

$$N(CN) = 3.43 \times 10^{13} T_A{}^* \Delta V \times [\![Q(T_{01}) / \{[J(T_{01}) - J(2.7)] \times [1 - \exp(-h\nu/kT_{01})]\}]\!], \quad (5)$$

where $T_A{}^*$, ΔV, ν, and T_{01} are the peak temperature, line width, frequency, and excitation temperature, respectively, for the strongest hyperfine component. The Einstein A-coefficient needed in this calculation was drawn from TG. In using equation (5), we have assumed that the populations of the rotational levels, and of the individual hyperfine levels within each rotational level, are in LTE, and that the CN-emitting region fills the telescope beam.

Two-level excitation calculations (which usually underestimate the value of T_{01}) were made for CN for various kinetic temperatures T_k and molecular hydrogen densities. A general result is that, for $T_k = 10$–16 K and molecular hydrogen volume density $[H_2] = 5 \times 10^3$ to 1×10^5, $T_{01} = 2.8$–7 K, with a strong dependence on the choice of the CN–H_2 collisional cross section. The physical conditions of dark clouds in which several molecular species have been observed and of the denser diffuse clouds are covered by these parameter ranges. In that case, the factor in braces in equation (5) may be equated to 1.2, the resulting error being no more than a factor of 2. For the two clouds in which the two strongest hyperfine components were detected, analyses of the relative line intensities suggest that the optical depths of the weaker components are $\lesssim 1$. Since the stronger components are optically thick, the values for N(CN) calculated in the above manner will be about a factor of 3 too small. The results for N(CO), N(CN), and N(CN)/N(CO) for the dark and diffuse clouds for which CO data are available are given in Table 5.

The results of two-level excitation calculations for the hotter, denser black clouds and circumstellar clouds suggest that the CN excitation temperature may run from 3 to 60 K. In this case, the factor in braces in equation (5) may again be replaced by 1.2, the error being no more than a factor of 2. Our LTE value of N(CN) for Orion A is in agreement with the result of TG's more sophisticated calculations to within a factor of 2. For both IRC +10216 and CIT 6, we have assumed that the CN- and CO-emitting regions are coextensive, which may well not be the case. Morris (1975) has shown that excitation conditions lead to a larger CO envelope for IRC +10216 than exists for the higher excitation molecules; such a condition may prevail for CIT 6 also. Thus our computed values of N(CN)/N(CO) may be lower limits. For Sgr B2 (OH), the CO column densities were derived from the line profiles of Scoville, Solomon, and Penzias (1975): the ^{13}CO optical depth was taken to be that at the profile peak. Since peculiar abundance and excitation variations exist in Sgr B2 (see below), this number is likewise uncertain, and our value may again be an underestimate of N(CN)/N(CO). The CN and CO column densities and the CN/CO relative abundances for these four clouds are presented in Table 5.

In certain regimes of kinetic temperature and cloud density, the CN collision cross sections $\sigma(\Delta N \geq 2)$ may be sufficiently large to result in an elevation of T_{01} or even an inversion in the populations of the $N = 0$ and $N = 1$ rotational levels (as demonstrated by Goldsmith 1972 in the case of CO). This would result in significant overestimates of N(CN) when calculated by the approach used in this paper. However, a simple multilevel calculation (M. Guélin, private communication) suggests that this occurs, if ever, only for the values of density and temperature usually associated with Orion A. The CN spectrum (cf. Fig. 2) for this region, on the other hand, shows no indication of unusual excitation.

TABLE 5

DERIVED CO AND CN ABUNDANCES

Source	V_{LSR} (^{12}CO) (km s^{-1})	T_{01} (^{12}CO) (K)	τ (^{13}CO)	N (^{13}CO) (cm^{-2})	N (^{12}CO)* (cm^{-2})	N (CN) (cm^{-2})	N (CN)/ N (CO)
a) Dark Clouds							
L1333	...	7.7	1.44	4.85 (+15)	4.32 (+17)	< 1.45 (+13)	< 2.6 (−5)
IC 1848-1	...	14.6	0.22	7.30 (+15)	6.50 (+17)	4.88 (+13)	7.5 (−5)
L1551	6.4	12.0	0.82	6.94 (+15)	6.18 (+17)	< 2.14 (+13)	< 3.4 (−5)
	−1.1	...	...	...	> 1.32 (+16)	...	...
L1529	...	10.9	0.99	1.09 (+16)	9.73 (+17)	1.35 (+13)	1.4 (−5)
L1534	...	10.4	0.51	6.53 (+15)	5.81 (+17)	< 3.52 (+13)	< 6.1 (−5)
L1552	...	10.6	0.58	3.96 (+15)	3.52 (+17)	< 1.69 (+13)	< 4.8 (−5)
Ori-I-2	...	13.0	0.48	5.16 (+15)	4.55 (+17)	2.22 (+13)	4.9 (−5)
L1622	1.0	17.2	0.66	1.16 (+16)	1.02 (+18)	< 2.04 (+13)	< 2.0 (−5)
	10.5	...	...	...	> 4.30 (+15)	...	...
B227	−0.5	9.4	0.55	3.68 (+15)	3.28 (+17)	< 1.63 (+13)	< 5.0 (−5)
	8.2	...	...	...	> 7.17 (+15)	...	...
Mon	8.2	14.0	0.57	1.23 (+16)	1.09 (+18)	< 2.03 (+13)	< 1.8 (−5)
	5.8	11.3	0.34	3.93 (+15)	3.49 (+17)	...	...
L134	...	8.0	1.52	6.50 (+15)	5.78 (+17)	< 2.06 (+13)	< 3.6 (−5)
L134 N	...	7.6	0.88	4.22 (+15)	3.76 (+17)	< 3.61 (+13)	< 9.6 (−5)
ρ Oph	...	12.5	0.23	7.91 (+15)	7.04 (+17)	< 5.63 (+13)	< 8.0 (−5)
Kh 3	...	6.3	0.16	2.71 (+15)	2.41 (+17)	< 9.82 (+13)	< 4.1 (−4)
B335	...	7.9	1.11	3.11 (+15)	2.77 (+17)	1.15 (+13)	4.2 (−5)
Cep C	...	14.7	0.62	1.53 (+16)	1.36 (+18)	< 3.54 (+13)	< 2.6 (−5)
b) Black Clouds							
Ori A	...	...	...	...	1.2 (+19)	6.13 (+14)	5.1 (−5)
Sgr B2 (OH)	...	...	...	...	7.5 (+19)	3.41 (+14)	4.6 (−6)
c) Circumstellar Clouds							
IRC +10216	...	...	...	...	3.7 (+17)	1.02 (+15)	2.8 (−3)
CIT 6	...	...	...	...	1.2 (+18)	1.06 (+14)	8.8 (−5)

NOTE.—1.0(+10) = 1.0 × 10^{10}.

* Derived assuming $N(^{12}CO)/N(^{13}CO) = 89$.

c) *Comments on the Observational Results*

The CN and CO column densities given in Table 5 will be discussed in the next section, with particular emphasis on their relation to dark cloud chemistry. Superficial examination of the data given in Tables 2–4 and depicted in Figures 1 and 2 reveals several interesting sidelights, and we conclude this section with a discussion of these.

The first is an apparent systematic velocity difference between the centers of the CO and ^{13}CO lines for dark clouds (Table 2), in the sense that the ^{13}CO lines have slightly higher velocities, the difference being largest for the narrowest lines. To check whether this effect is real or not, we have examined three other dark cloud surveys: those of Dickman (1975), velocity resolution 0.65 km s^{-1}; of Milman *et al.* (1975*a*, *b*), velocity resolution 0.27 km s^{-1}; and of Knapp (1977), velocity resolution 0.65 km s^{-1}. In none of these cloud surveys is such an effect apparent. Moreover, additional observations of some of the clouds by R. Martin (private communication) did not show such velocity variations. We must therefore conclude that the effect is instrumental (although we have carefully checked through our data for any errors, for example, in the value of the intermediate frequency), and intrinsic to the NRAO system as we used it. Thus our quoted velocities are inaccurate to at least 0.5 km s^{-1}. The values of the velocities are not important for our present work, and we assume in the next section that the CO-, ^{13}CO-, and CN-emitting regions are in fact cospatial.

A second point is the high velocity (90 km s^{-1}; see Table 4) for the CN lines toward Sgr B2. Most of the high-excitation molecules peak at ~64 km s^{-1}. However, the most abundant (CO, CS, HCN) emit over a very wide velocity range and have their most intense emission at ~90 km s^{-1} (see Scoville, Solomon, and Penzias 1975). Our result suggests chemical differences between the 64 and 90 km s^{-1} cloud, with CN having a very high abundance in the latter region. More sensitive observations of CN in Sgr B2 would be very valuable, as well as mapping observations to determine its spatial extent.

Of the dark clouds observed, only four were detected (see Table 2). In two of these, L1529 and Ori I-2, we also detected the second strongest hyperfine component. The ratio of the two components in each case suggests that the CN line is saturated in these clouds, although the signal-to-noise ratio for this observation, as for all of our dark cloud CN work, is quite poor. If the CN line is partially saturated, the excitation temperature T_{01} cannot be much larger than 4 K, which reinforces our adoption of densities too low to thermalize the CN transitions (the kinetic temperature is 11 K for this cloud: see Table 5). Since the CN lines which we have detected are all very weak, not much larger than the 3 σ upper limits for the undetected clouds, it may be that CN can be detected much more widely in dark clouds with an increase in system sensitivity of about a factor of 2.

There are several discrepancies between our diffuse cloud results and those published by TG and Knapp and Jura (1976). Since an image sideband rejection filter was utilized in the present work, resulting in an elimination of those calibration errors that will occur in the double-sideband observing mode due to the unbalanced response functions of the different sidebands, our line parameters are probably more accurate than those given in TG for the same sources. In particular, their reported detection of CN toward HD 21483 ($T_A{}^* \sim 0.55$ K) is not confirmed by the present observations ($T_A{}^* < 0.35$ K). On the other hand, our upper limit for CN toward HD 154368 does not contradict the weak detection of TG. Toward HD 21483, our CO column density is quoted for the 6 km s^{-1} component; that given by Knapp and Jura is for the 2 km s^{-1} wing. In fact, the 6 km s^{-1} component arises from a dark cloud, the large Perseus dust cloud, which lies *behind* HD 21483; the interstellar absorption lines in HD 21483 are at 2 km s^{-1}. The CO profile of Knapp and Jura (1976) shows a wing on the ^{12}CO line extending to ~ 0 km s^{-1} at a level of ~ 0.8 K. This was not detected in the present work, because the signal-to-noise ratio was probably too poor to see it. All in all, our diffuse cloud observations show that millimeter-wavelength emission from CN is generally not detected from these clouds, although CO emission is sometimes found.

III. COMPARISON OF THEORETICAL MODELS WITH OBSERVATIONAL RESULTS

Since the chemistry may vary among cloud types, we have grouped our observational results appropriately and will consider them separately. Implicit in any comparison of the column densities of different molecules is the assumption that the molecular line emitting regions are cospatial. In the case of ^{13}CO and CN, this seems to be a reasonable assumption because the detected CN lines generally have the same velocity and velocity widths as the ^{13}CO lines in the same sources. The CO lines are broader than these, but this is to be expected because of saturation effects. Thus, it can generally be assumed that the CO and CN regions are well mixed.

a) *Dark Clouds*

Emission from CN was detected in the direction of four dark clouds: IC 1848-1, L1529, Ori-I-2, and B335. These detections indicate that both a sufficient gas density for $T_{01} > T_{bg}$ *and* sufficient column density to produce a detectable signal exist in these directions. The fact that CN was not observed in the other dark clouds, on the other hand, does not necessarily mean that insufficient density for excitation exists in these clouds. In fact, high-excitation molecular transitions have been detected in many of these clouds: H_2CO 2 mm transitions in L1529 and L134 N (Evans and Kutner 1976), ρ Oph (Evans *et al.* 1978), and Cepheus C (Sargent 1977), and HCN in L134 (Snyder and Hollis 1976), L1529, L1534, L1551, and B335 (Allen and Dickman 1978). Since the *A*-coefficient for the strongest CN line is smaller than or equal to that of the 1–0 HCN lines or the 2 mm H_2CO lines, it is likely that a number of the other dark clouds in which CN was not observed may also have been sufficiently dense to excite T_{01} above T_{bg}. Total gas column density is also not the limiting factor, since most of the clouds in which CN was not seen have CO column densities equal to, or greater than, the clouds in which CN was detected. All of this suggests that the CN/CO abundance ratio differs among dark clouds with otherwise similar properties.

The relative CN to CO abundance ratios for the clouds in which CN was detected range from 1.4×10^{-5} to 7.5×10^{-5}. Considering the various approximations used in making these calculations (§ II*b*), the N(CN)/N(CO) ratio may sometimes have been underestimated by as much as a factor of 3. Thus, this spread may not be real. Indeed, the two strongest hyperfine components were observed toward L1529 [which has the lowest calculated value for N(CN)] and Ori-I-2. In these clouds, N(CN) *will* have been underestimated. On the other hand, the largest observed relative abundance is in the direction of IC 1848-1, an H II region in front of a dark cloud. Since in this source the CO and CN lines are 2.7–3.3 km s^{-1} wide whereas the CS lines are 1.7–1.9 km s^{-1} wide, it is possible that the CS emission arises from the cold interior of the background dark cloud while the CO and CN signals come from the cloud adjacent to, and heated by, the H II region. If this is the case, the IC 1848-1 results should be interpreted as for black clouds, and not dark clouds.

The observed abundances may be compared with those predicted by the various theoretical chemical models of dark clouds. In Table 6, we summarize the different models and give the predicted CN/CO abundance ratios (square brackets indicate volume density). Taking 5×10^{-5} as a typical observed value for N(CN)/N(CO) in dark clouds, it can be seen from Table 6 that the model of Watson and Salpeter (1972) is clearly not efficient enough in dense, dark clouds to explain the observed abundances. On the other hand, the pure gas-phase collapse model of Suzuki *et al.* (1976) and the time-dependent gas-phase model of PH at 10 K produce too much CN relative to CO and therefore require more CN depletion, possibly on grain surfaces, to be reasonable possibilities. Similarly, the Pickles and Williams (1977) model, which includes both gas-phase and grain surface reactions, predicts a value for [CN]/[CO] significantly in excess of observations, the overproduction of CN being a problem

TABLE 6

THEORETICAL INTERSTELLAR CHEMICAL MODELS

Model	Chemical Processes	Parameters	[CN]/[CO]
		Dark and Black Clouds	
Watson and Salpeter 1972	Gas-phase and surface reactions; photoprocesses included	Optical depth at 1000 Å = 12.5	
		[H] = 10^4 cm^{-3}, ξ = 2.7 × 10^7	3.7 (−9)
		[H] = 10^5 cm^{-3}, ξ = 2.7 × 10^8	3.7 (−10)
Herbst and Klemperer 1973	Gas-phase, predominantly ion-molecule, reactions	ζ = 10^{-17} s^{-1}, O/H = 4.4 × 10^{-4} {6.8 × 10^{-4}}	
		[H_2] = 10^4 cm^{-3}	6.7 (−5) {5.3 (−6)}
		[H_2] = 10^5 cm^{-3}	5.3 (−6) {5.3 (−8)}
		[H_2] = 10^6 cm^{-3}	5.3 (−7) {5.3 (−10)}
Suzuki *et al.* 1976	Gas-phase reactions; photoprocesses included	Collapse parameter = 10	
		[H] = 10^4 cm^{-3}	1.0 (−2)
		[H] = 10^5 cm^{-3}	1.3 (−2)
		[H] = 10^6 cm^{-3}	1.3 (−2)
Allen and Robinson 1977	Surface reactions	$T_{gr} = T_k$ = 10 K	
		[H(0)] = 10^4 cm^{-3}, t = 10^6 {10^7} yr	1.4 (−1) {6.7 (−3)}
		[H(0)] = 10^5 cm^{-3}, t = 10^6 {10^7} yr	7.9 (−3) {0}
		T_k = 70 K, [H(0)] = 2 × 10^6 cm^{-3}, t = 10^5 yr	7.9 (−6)
Prasad and Huntress 1978	Gas-phase reactions	[H_2] = 4 × 10^5 cm^{-3}, O/H = 1.8 × 10^{-4}	
		T = 10 K, t = 10^6 {10^7} yr	6.6 (−2) {4.6 (−2)}
		T = 60 K, t = 10^6 {10^7} yr	2.5 (−6) {3.2 (−5)}
Iglesias 1977	Predominantly gas-phase ion-molecule reactions	T = 30 K	
		H:O:C:N = 1:1.8 (−4):7.3 (−5):2.1 (−5) {1:4.4 (−4):3.75 (−4):8.7 (−5)}	
		[H + $2H_2$] = 2 × 10^4 cm^{-3}, t = 10^5, 10^6, 10^7 yr	4.5 (−3), 3.6 (−4), 1.4 (−5) {3.7 (−3), 1.0 (−2), 1.0 (−5)}
		with grain condensation	
		t = 10^5, 10^6 yr	4.9 (−3), ?
		[H + $2H_2$] = 2 × 10^6 cm^{-3}, t = 10^5, 10^6, 10^7 yr	6.5 (−5), 2.1 (−6), 8.3 (−8)
Pickles and Williams 1977	Gas-phase and surface reactions; photoprocesses included	$\tau_v \gtrsim 9$, T = 10–20 K,	
		[H + $2H_2$] = 2 × 10^4 cm^{-3}	∼8 (−1)
		Circumstellar Clouds	
Tsuji 1964	Thermal dissociation	C/O = 5, N/C = 10, P_g ∼ 1 atm	
		T = 1008 K	1.7 × 10^{-9}
		T = 1260 K	2.3 × 10^{-6}
		T = 1680 K	3.5 × 10^{-3}
		T = 2520 K	3.7 × 10^{-1}

NOTES.—Refer to individual references for exact definitions of symbols. 1.0 (+10) = 1.0 × 10^{10}.

noted by the authors themselves. The gas-phase, ion-molecule reaction scheme proposed by HK, however, does fit the observations quite well, although there is a question as to what is the appropriate overall O/H ratio to use; the results are very sensitive to the particular choice of this ratio. Less sensitive to the particular value of the O/H ratio, the more recent time-dependent gas-phase IG model matches the observed N(CN)/N(CO) ratio quite well for reasonable values of cloud age. But when grain condensation is included as a loss mechanism, all molecules are depleted onto the grains on time scales of a few times 10^5 years, possibly much shorter than cloud ages. On the other hand, the grain reaction model of AR77 (which includes loss through depletion onto grains) for clouds for which the total hydrogen abundance (i.e., [H(t = 0)]) is $\gtrsim 2 \times 10^4$ cm^{-3} will also be in accord with observations, depending on the age of the cloud. Thus the present observations do not clearly distinguish between gas-phase and grain surface reactions as the sources of CN in dark clouds.

In concluding this section, it is interesting to consider, as suggested before, what the nondetection of CN in clouds with physical conditions seemingly similar to clouds in which it was detected reveals about the nature of dark cloud chemistry. In the case of the HK model, the N(CN)/N(CO) ratio decreases with increasing H_2 density, the decrease being most precipitate for the O/H ratio presently taken as the "cosmic" value (Cameron 1973). On the other hand, if further observations find that the densities of these clouds are all very similar, a better explanation for the relative abundance variations may be derived from the time-dependent models of AR77 and IG, in which CN becomes depleted relative to CO as a moderately to very dense cloud ages. Likewise AR76 suggest that the observed fraction of hydrogen in atomic form may be a function of cloud age and cloud density, and they derive ages for a number of clouds observed by Knapp (1974). Unfortunately only one cloud analyzed by AR76 was in our observational sample—L1534. AR76 determined the age of L1534 to be $\gtrsim 10^7$ years, so that nondetection of CN is not inconsistent if L1534 is more dense than their estimate of 2.8×10^3 cm^{-3}. Another cloud in our study, B227, has been recently observed in H I by Martin and Barrett (1976). The H I self-absorption detection yields a fractional abundance for atomic hydrogen, $f_H = 2.4 \times 10^{-3}$ to 2.5×10^{-2}, with the value for $N(H + 2H_2)$ derived from our observations of ^{13}CO and $N(^{13}CO)/N(H_2) = 2 \times 10^{-6}$ (Dickman 1977). The density of the cloud can be estimated from the angular diameter suggested in Rickard *et al.* (1977), yielding a cloud age of $\sim 10^7$ years also. In a similar manner, the H I data for L1551 and L1552 (Knapp 1974) can be analyzed, and cloud ages similar to that of B227 result. The CN radical was not detected in any of these sources. It would be interesting to obtain H I results for the clouds in which CN was observed to see whether the calculated cloud ages are significantly less than those of the four clouds just discussed.

b) *Black Clouds*

The hyperfine components in Orion A are resolved, and the simultaneous fit of the multiplet in the optically thin case is very good (Fig. 2). TG also conclude that CN in Orion A is optically thin, but their antenna temperatures are smaller than our values. The N(CN)/N(CO) ratio (within a factor of 2 of that of TG) is comparable to the ratios in the dark clouds, although other observations suggest that the physical conditions are significantly different. Of the models presented in Table 6 that are appropriate to black clouds, the higher density gas-phase IG model best fits the Orion A result; the higher temperature gas-phase PH model and the high-density, high-kinetic-temperature (T_k = 70 K) grain reaction model of AR77 less so; and the high-density gas-phase calculations of HK least of all. There is still the question of the appropriate O/H abundance ratio, the different models varying as to their choice, with the results of HK showing an increasing sensitivity to the adopted value with increasing gas density.

The present observations confirm the existence of CN in Sgr B2(OH); the spectral line feature was initially detected by Kuiper *et al.* (1977) but left without certain identification due to the indeterminacy of the sideband. Since the line profile is synthesized well by a multiplet of Gaussian functions (Fig. 2), one for each hyperfine component, with identical velocities and line widths, the origin of the line feature is reasonably clear. The value of N(CN)/N(CO) is significantly smaller than that for Orion A. In § II we discuss several sources of uncertainty in the calculation of this number. If cloud age is taken as a relatively free parameter, the medium density (initial hydrogen atom concentration [H(O)] = 10^5 cm^{-3}) model of AR77 and the models of PH and IG can account for the Sgr B2 value. The HK results also seem to be in reasonable agreement, again depending on the adopted O/H ratio. As is the case for dark clouds, the black cloud results for the CN/CO abundance ratio cannot be unambiguously interpreted in terms of a particular chemical reaction theory.

c) *Circumstellar Clouds*

Emission due to CN was detected in IRC +10216 and CIT 6 (Fig. 2). The result for CIT 6 is a new detection, whereas TG had previously detected CN in IRC +10216, although their reported antenna temperature is significantly lower than ours. The line parameters (velocity and velocity width) derived for CN, assuming that all the hyperfine components are optically thin, match well those reported for CO by others (Kuiper *et al.* 1976; Mufson and Liszt 1975).

In these circumstellar clouds CN seems to be up to 100 times more abundant relative to CO than in the other interstellar cloud types. Indeed, the molecular clouds surrounding carbon stars, most notably IRC +10216, previously have been observed to be rich in molecules containing carbon and nitrogen atoms (HC_3N, Morris *et al.* 1975; C_3N, Guélin and Thaddeus 1977). These observations might best be explained by the following model. Gas and dust expelled from the atmosphere of the underlying carbon star provide the material for the circumstellar cloud. The relative abundances of the molecular component of the outflowing gas may reflect the stellar physical conditions under which the molecules were formed if the outflow time scales are shorter than the appropriate time scales for further reaction and if the ambient ultraviolet field is sufficiently weak that photodissociation is minimal. In such a manner, Morris (1975) interprets his observations of SiS and SiO in IRC +10216 as resulting from a 2000 K carbon-rich stellar atmosphere. In the case of CN, as shown in Table 6, the equilibrium calculations of Tsuji (1964) for a carbon-rich, nitrogen-rich atmosphere in the temperature range 1400–1700 K are in good agreement with the circumstellar cloud observations. The fact that the chemical models proposed for several of the other cloud types also predict a high N(CN)/N(CO) ratio under certain conditions leaves ambiguous the identification of the precise nature of circumstellar cloud chemistry.

IV. SUMMARY AND CONCLUSIONS

We have searched for emission from interstellar CN at 113 GHz in a variety of interstellar clouds: in dark dust clouds, diffuse clouds, the circumstellar envelopes of the late-type stars CIT 6 and IRC +10216, and in the dense black molecular clouds in Orion A and Sgr B2. The CN radical was detected in four of the dark clouds, in none of the diffuse clouds, and in all of the last four objects; this is the first detection of CN in dark clouds. The CN column densities are typically 10^{13} mol cm^{-2}.

As a comparison molecule, we also observed the $J = 1 \rightarrow 0$ transitions of CO and ^{13}CO in the same directions, since these molecules give a fairly good estimate of total gas column density. We found that the relative abundance of CN in dark clouds shows possibly statistically significant variations in otherwise similar clouds. Time-dependent interstellar chemical models can directly explain such variation as reflecting cloud age. The values for N(CN)/N(CO) in dark clouds do not clearly indicate the type of chemistry occurring—gas-phase versus grain surface reactions—since there are a number of free parameters in each of the published models which strongly affect the predictions.

The CN/CO abundance ratio in the Orion A molecular cloud is similar to that in dark clouds, but that in the Sgr B2 cloud is significantly smaller. Moreover, the CN emission occurs at an unusual velocity in this latter region, at +90 km s^{-1}, and may thus be present in only one part of the cloud, with chemical differences existing throughout the cloud. Again the nature of the chemistry cannot be unambiguously determined from the CN/CO results.

The abundances of CN in the envelopes of the evolved stars CIT 6 and IRC +10216 are on the average much higher than elsewhere, as is appropriate for evolved molecular envelopes. Other carbon- and nitrogen-rich molecules have been observed in these regions (e.g., Morris 1975).

The sensitivity used in the present work, while the highest available at present, is not sufficient to provide detailed comparisons of observations with theory. However, our present limited results have suggested that the variability of CN abundance in interstellar clouds is a potentially powerful tool for elucidating interstellar chemistry.

We thank the National Radio Astronomy Observatory for the observing time to carry out this project. We are very grateful to R. L. Dickman, M. Guélin, W. Huntress, R. N. Martin, S. Prasad, B. Turner, and B. L. Ulich for assistance provided during the course of this work. Financial support was provided by the National Science Foundation through NRAO and through grant AST 73-04677 A03 to the Owens Valley Radio Observatory. M. Allen would also like to acknowledge support as an NRC-NASA Resident Research Associate.

REFERENCES

Allen, M., and Dickman, R. L. 1978, in preparation.
Allen, M., and Robinson, G. W. 1976, *Ap. J.*, **207**, 745 (AR76).
———. 1977, *Ap. J.*, **212**, 396 (AR77).
Cameron, A. G. W. 1973, *Space Sci. Rev.*, **15**, 121.
Dickman, R. L. 1975, *Ap. J.*, **202**, 50.
———. 1977, preprint.
Dixon, T. A., and Woods, R. C. 1977, *J. Chem. Phys.*, **67**, 3956.
Evans, N. J., Knapp, G. R., Loren, R. B., and Lo, K. Y. 1978, in preparation.
Evans, N. J., and Kutner, M. L. 1976, *Ap. J.* (*Letters*), **204**, L131.
Gerola, H., and Glassgold, A. E. 1978, *Ap. J.*, **221**, 717.
Goldsmith, P. F. 1972, *Ap. J.*, **176**, 597.
Guélin, M., and Thaddeus, P. 1977, *Ap. J.* (*Letters*), **212**, L81.
Herbst, E., and Klemperer, W. 1973, *Ap. J.*, **185**, 505 (HK).
Iglesias, E. 1977, *Ap. J.*, **218**, 697 (IG).
Knapp, G. R. 1974, *A.J.*, **79**, 527.
———. 1977, in preparation.
Knapp, G. R., and Jura, M. 1976, *Ap. J.*, **209**, 782.
Kuiper, E. N. R., Kuiper, T. B. H., Zuckerman, B., and Kakar, R. K. 1977, *Ap. J.*, **214**, 394.
Kuiper, T. B. H., Knapp, G. R., Knapp, S. L., and Brown, R. L. 1976, *Ap. J.*, **204**, 408.
Langer, W. D., and Glassgold, A. E. 1976, *Astr. Ap.*, **48**, 395.
Lucas, R. 1974, *Astr. Ap.*, **36**, 465.
Martin, R. N., and Barrett, A. H. 1975, *Ap. J.* (*Letters*), **202**, L83.
———. 1976, *B.A.A.S.*, **8**, 498.
Milman, A. S., Knapp, G. R., Kerr, F. J., Knapp, S. L., and Wilson, W. J. 1975*a*, *A.J.*, **80**, 93.
Milman, A. S., Knapp, G. R., Knapp, S. L., and Wilson, W. J. 1975*b*, *A.J.*, **80**, 101.
Morris, M. 1975, *Ap. J.*, **197**, 603.
Morris, M., Gilmore, W., Palmer, P., Turner, B. E., and Zuckerman, B. 1975, *Ap. J.* (*Letters*), **199**, L47.
Mufson, S. L., and Liszt, H. S. 1975, *Ap. J.*, **202**, 183.
Oppenheimer, M., and Dalgarno, A. 1975, *Ap. J.*, **200**, 419.
Pickles, J. B., and Williams, D. A. 1977, *Ap. Space Sci.*, **52**, 453.
Prasad, S., and Huntress, W. 1978, in preparation (PH).
Rickard, L. J, Palmer, P., Buhl, D., and Zuckerman, B. 1977, *Ap. J.*, **213**, 654.
Sargent, A. I. 1977, *Ap. J.*, **218**, 736.

Scoville, N. Z. 1972, Ph.D. thesis, Columbia University.
Scoville, N. Z., and Solomon, P. M. 1974, *Ap. J. (Letters)*, **187**, L67.
Scoville, N. Z., Solomon, P. M., and Penzias, A. A. 1975, *Ap. J.*, **201**, 352.
Snyder, L. E., and Hollis, J. M. 1976, *Ap. J. (Letters)*, **204**, L139.
Suzuki, H., Miki, S., Sato, K., Kiguchi, M., and Nakagawa, Y. 1976, *Progr. Theoret. Phys.*, **56**, 1111.
Turner, B. E. 1974, in *Galactic and Extra-galactic Radio Astronomy*, ed. G. L. Verschuur and K. I. Kellermann (New York: Springer-Verlag), p. 199.
Turner, B. E., and Gammon, R. H. 1975, *Ap. J.*, **198**, 71 (TG).
Tsuji, T. 1964, *Ann. Tokyo Astr. Obs.*, 2d Ser., **9**, 1.
Ulich, B. L., and Haas, R. W. 1976, *Ap. J. Suppl.*, **30**, 247.
Wannier, P. G., Arnaud, J. A., Pelow, F. A., and Saleh, A. A. M. 1976*a*, *Rev. Sci. Instrum.*, **47**, 56.
Wannier, P. G., Penzias, A. A., Linke, R. A., and Wilson, R. W. 1976*b*, *Ap. J.*, **204**, 26.
Watson, W. D., and Salpeter, E. E. 1972, *Ap. J.*, **175**, 659.
Zuckerman, B., and Palmer, P. 1974, *Ann. Rev. Astr. Ap.*, **12**, 279.

MARK ALLEN: Division of Geological and Planetary Sciences, California Institute of Technology, Pasadena, CA 91125

GILLIAN R. KNAPP: Owens Valley Radio Observatory, California Institute of Technology, Pasadena, CA 91125